PAPER

Decoding sign language finger flexions from high-density electrocorticography using graph-optimized block term tensor regression

Journal of Neural Engineering

PAPER

Decoding sign language finger flexions from high-density electrocorticography using graph-optimized block term tensor regression

Axel Faes[1,*], Eva Calvo Merino[1], Mariana P Branco[2], Anaïs Van Hoylandt[3], Elina Keirse[3], Tom Theys[3], Nick F Ramsey[2] and M M Van Hulle[1]

[1] KU Leuven—University of Leuven, Department of Neurosciences, Laboratory for Neuro- & Psychophysiology, B-3000 Leuven, Belgium
[2] UMC Utrecht Brain Center, Department of Neurology & Neurosurgery, University Medical Center Utrecht, Utrecht, The Netherlands
[3] KU Leuven—University of Leuven, Department of Neurosciences, Research Group Experimental Neurosurgery and Neuroanatomy, B-3000 Leuven, Belgium
[*] Author to whom any correspondence should be addressed.

E-mail: axel.faes@kuleuven.be

Keywords: BTTR, finger, gestures, sign language, ECoG, regressions

RECEIVED
28 August 2023

REVISED
6 January 2025

ACCEPTED FOR PUBLICATION
16 April 2025

PUBLISHED
24 April 2025

Abstract

Objective. A novel method is introduced to regress over the sign language finger movements from human electrocorticography (ECoG) recordings. *Approach.* The proposed graph-optimized block-term tensor regression (Go-BTTR) method consists of two components: a deflation-based regression model that sequentially Tucker-decomposes multiway ECoG data into a series of blocks, and a causal graph process (CGP) that accounts for the complex relationship between finger movements when expressing sign language gestures. Prior to each regression block, CGP is applied to decide which fingers should be kept separate or grouped and should therefore be referred to BTTR or its extended version eBTTR, respectively. *Main results.* Two ECoG datasets were used, one recorded in five patients expressing four hand gestures of the American sign language alphabet, and another in two patients expressing all gestures of the Flemish sign language alphabet. As Go-BTTR combines fingers in a flexible way, it can better account for the nonlinear relationship ECoG exhibits when expressing hand gestures, including unintentional finger co-activations. This is reflected by the superior joint finger trajectory predictions compared to eBTTR, and predictions that are on par with BTTR in single-finger scenarios. For the American sign language alphabet (Utrecht dataset), the average correlation across all fingers for all subjects was 0.73 for Go-BTTR, 0.719 for eBTTR and 0.70 for BTTR. For the Flemish sign language alphabet (Leuven dataset), the average correlation across all fingers for all subjects was 0.37 for Go-BTTR, 0.34 for eBTTR and 0.33 for BTTR. *Significance.* Our findings show that Go-BTTR is capable of decoding complex hand gestures taken from the sign language alphabet. Go-BTTR also demonstrates computational efficiency, providing a notable benefit when intracranial electrodes are inserted during a patient's pre-surgical evaluation. This efficiency helps reduce the time required for developing and testing a brain–computer interface solution.

1. Introduction

Millions of individuals experience paralysis. This can be the result from a spinal cord injury due to, for instance, an accident. It can also occur from brainstem stroke, or from progressive disorders like amyotrophic lateral sclerosis (ALS) [1]. Various assistive technologies have been proposed to provide an alternative means of communication (for a review see [2]), including brain computer interfaces (BCIs) used, among others, to select letters one-by-one to spell out words. Motor BCIs bypass the muscles of the human body and can thus be used to restore the function of, or replace those muscles. As discussed in [3], electrical stimulation can be an example of such a system. The stimulation occurs in the regions

of the hand-knob area and the relevant spinal cord regions associated with walked. Additionally, BCIs contribute to the control of external limbs, such as prosthetic hands in case of full replacement, or exoskeletons in case of supporting existing function, or other effectors, as demonstrated in works such as [4–7]. Over the last few decades, electrocorticography (ECoG) has been gaining attention in the BCI research community, which involves electrodes placed on top of the cortical surface to record electrical activity. When ECoG signals are recorded from the primary motor cortex, they reveal notable motor-related spatio-temporo-spectral patterns that can be leveraged to capture the dynamics of the corresponding movement, as discussed in works such as [8–10]. However, decoding rapid and coordinated finger movements, as in grasping and performing hand gestures, is challenging, calling for further algorithmic developments.

Ramsey and colleagues successfully classified four gestures based on hand motor ECoG recordings in two subjects. These gestures were taken from the American sign language alphabet. By extracting the local motor potentials (LMPs) for each channel and using temporal template matching, classification was accomplished, as described in [11]. Li *et al* [12] classified three gestures ('scissors,' 'rock,' and 'paper') from hand motor ECoGs in two participants using an SVM-based classifier achieving 80% accuracy on average in three participants. The classification results were also translated into commands for controlling a prosthetic hand in two participants. Pan *et al* [13] classified the same three gestures but used a recurrent neural network (RNN) that exploits the temporal information present in the ECoG recordings thereby achieving 90% accuracy in two participants.

Within regression analysis, multiway approaches are being applied more and more. As discussed in works such as [14, 15], they are used to model arm trajectories from ECoG signals recorded from monkeys. Additionally, these approaches have been utilized in the context of exoskeleton-based arm trajectory, arm- and wrist rotations, and ECoG signals in tetraplegic patients, as highlighted in [16]. Furthermore, multiway methods have been employed in the study of graded stimulation of the spinal cord region involved in walking in tetraplegic patients, as presented in [3]. In the latter two scenarios, multiway partial least squares regression (NPLS) or a variation thereof is used within the decoders. However, this approach falls short in achieving the required level of accuracy for decoding fine finger movements, as discussed in [16]. This limitation may be attributed to factors such as limited fitness capacity, high computational complexity, and slow convergence of NPLS, particularly when dealing with higher-order data, as highlighted in [14]. On a more promising note, Zhao *et al* [14] have introduced a robust generalized framework known as higher-order partial least squares (HOPLS). This framework is founded on a $(1, L_2, \ldots, L_N)$-rank block term decomposition (BTD), where all blocks share the same multilinear rank, referred to as multilinear tensor rank (MTR). HOPLS provides an optimal balance between fitness and model complexity, resulting in enhanced predictability. Consequently, HOPLS has demonstrated superior performance compared to conventional partial least squares (PLS) approaches.

Camarrone and colleagues recently introduced block-term tensor regression (BTTR) as detailed in [17, 18]. BTTR is grounded in Tucker decomposition and incorporates a deflation scheme that generates a sequence of blocks, each contributing successively less to the regression performance. Importantly, these blocks can possess varying MTR ranks, and their parameters are optimized automatically and on a block-by-block basis using automatic component extraction (ACE). Notably, BTTR has demonstrated performance comparable to that of HOPLS, while significantly reducing training time. However, it is worth noting that, unlike HOPLS, BTTR is limited to predicting scalar variables. The aforementioned limitation becomes evident when decoding complex finger movements, which occur during actions such as grasping. A potential solution for avoiding this limitation is to employ an individual BTTR model for each finger. However, this approach imposes constraints on the utilization of shared information among the fingers. Moreover, in situations where multiple fingers are engaged in simultaneous flexion, the recorded signals demonstrate temporal overlap and spatial sparsity, as discussed in [13]. This presents a difficulty because exclusively training on individual finger movements might be inadequate for decoding the complexity of coordinated or multiple finger movements.

Faes *et al* recently proposed an extension of BTTR called eBTTR (extended BTTR) [19] to enable the prediction of coordinated finger flexions thereby also capturing finger co-activations, i.e. unintentional movements of other fingers. These co-activations are likely not encoded by the ECoG signal, but decoded by the eBTTR model as it is trained to replicate finger movements recorded with a data glove. However, as the recursive Tucker decomposition unfolds, some single-finger accuracies continue to improve but at the expense of other fingers, even to the extent that their accuracy becomes outperformed by that of (single-finger) BTTR. In order to remedy this divergence, graph-optimized BTTR (Go-BTTR) is proposed in which causal graph process (CGP) modeling [20] is applied prior to regression to determine which

fingers should be jointly regressed and which ones not. As a case study, we consider finger trajectory prediction when expressing 4 letters of the American sign language alphabet using an existing ECoG dataset [21], and when expressing all letters of the Flemish sign language alphabet using a newly recorded ECoG dataset. As the latter has never been attempted before, it could shed light on the feasibility of sign language as a BCI-based communication paradigm.

2. Materials and methods

2.1. Datasets and tasks

Our study utilized two distinct datasets. The first dataset had been previously employed for classifying four gestures taken from the American sign language alphabet, whereby the initial study received approval from the Medical Ethical Committee of the Utrecht University Medical Center [21]. In our current research, this dataset serves as the basis for regressing finger movement trajectories associated with these gestures. This dataset encompasses five patients (with age ranging from 19 to 45 with mean 31, as detailed in table 1). These individuals were diagnosed with intractable epilepsy and underwent the implantation of subdural ECoG grids to aid in localizing their epileptogenic zones. The implanted grids consisted of both standard clinical and high-density ECoG grids. The standard grids featured electrodes positioned at a 1 cm center-to-center inter-electrode distance with a 2.3 mm electrode diameter, sourced from AdTech, Racine, USA. The high-density grids were equipped with either 32 or 64 channels, utilizing a 1.3 mm electrode diameter and a 3 mm center-to-center inter-electrode distance, also sourced from AdTech, Racine, USA. The 32-channel grid covered an area of 2.5 cm^2 with a 4×8 electrode layout, while the 64-channel grid encompassed an area of 5.2 cm^2 with an 8×8 electrode layout. Notably, subject 1 was excluded from further analysis since there were no electrodes covering the M1 brain area.

The task, as detailed in [11], required participants to perform four distinct hand gestures. In this study, these gestures were derived from the American sign language alphabet, as shown in figure 1. Specifically, participants were instructed to replicate the displayed gesture and maintain it for a duration of 6 s. Each of the trials included intervals of rest lasting 6 s. During these rest periods, participants were instructed to maintain an open hand position. Each experimental run consisted of 40 gesture trials (with each gesture repeated ten times in random order) and 41 rest trials. Participant 5 underwent the experiment twice. All participants' gestures were recorded using a data glove from 5DT Inc. (Irvine, USA). Any incongruent or erroneous trials, such as incorrect gestures, extra finger movements, or gesture corrections, were excluded from subsequent analysis.

The second dataset originates from two patients with refractory neuropathic facial pain with epidural ECoG grids placed as part of their pain treatment (neuromodulation, motor cortex stimulation). The experiment involving this dataset received approval from the Ethics Committee Research UZ/KU Leuven (EC Research). The first patient was implanted with epidural ECoG grids on the right hand-knob area and the second patient was implanted with an epidural ECoG grid on the left subcentral gyrus and broca area and the right hand-knob area (see table 2).

Two tasks were performed (subject 2 only performed Task 2). The first task concerns single-finger movements. The first subject was given a cue to move a specific single finger whose trajectory was gauged with a data glove (5DT Inc. Irvine, USA). In total, 150 trials were executed in a singular session lasting 600 s with 30 trials for each finger. On average, subjects were tasked to flex the cued finger once for 1 to 2 s, after which was a rest period lasting 2 s. In the second task, the two subjects were cued to replicate one of the 26 letters of the Flemish sign language alphabet (see figure 1), presented in randomized order, with the finger trajectories gauged with the data glove. Since the experiment took place in Flanders (Belgium), the Flemish sign language alphabet was used.

2.2. Go-BTTR

2.2.1. Overview

Since BTTR can only predict the movement of a single finger, multiple finger models should be used in the case of a subject's hand, while eBTTR can predict their joint movement. This is visualized in figure 2. In order to decode complex gestures from multiway ECoG data in a stable manner, as eBTTR can exhibit unstable single-finger accuracies as the Tucker decomposition unfolds [19] (see also the Results section), we use a CGP [20]. First, CGP is applied to determine which fingers should be kept separate in the regression and which ones joined, as illustrated in the first iteration step of figure 3. In the first iteration, CGP finds that 2 fingers are connected (cf the bidirectional arrow) and that the remaining ones are unconnected. Then, single BTTR blocks are used for the prediction of the trajectories of the unconnected fingers individually and a single eBTTR block for the prediction of the trajectories of the two connected fingers. In this way, Go-BTTR provides a middle ground between both regression methods. In the case of figure 3, the first iteration step in Go-BTTR has one eBTTR and three BTTR blocks. There are two special cases of Go-BTTR, depending on the outcome of

Table 1. Patient information Utrecht dataset (adapted from [21]).

Patient	Subject 2	Subject 3	Subject 4	Subject 5
Age	42	19	19	45
Gender	Male	Female	Male	Female
Handedness	Right	Right	Right	Left
Implanted hemisphere	Left	Left	Left	Right
Epileptic resected area	Temporal lobe (including amygdala and hippocampus)	Posterior medial frontal gyrus until pre-central gyrus	Anterior temporal lobe (including amygdala and hippocampus)	Frontal-para-sagittal
High-density grid location	Hand knob (pre-central and superior post-central)	Hand knob (pre- and post-central)	Hand knob (superior pre-central)	Hand knob (primarily post-central)
Total number of included electrodes	24/32	32/32	31/32	59/64
Number of electrodes over M1	15	16	31	11
Number of electrodes over S1	9	16	—	48

Table 2. Patient information Leuven dataset.

Patient	Subject 1	Subject 2
Age	58	41
Gender	Female	Female
Handedness	Right	Right
Region of pain	Trigeminus neuralgia (left)	Temporomandibular joint disorder, bilateral pain mostly in jaws.
Number of grids	1	2
Type of grid	Medtronic Inc Specify® SureScan® MRI 5-6-5 grid (in-line spacing 4.5 mm, row spacing 1.0 mm, electrode size 4 mm)	2X Medtronic Inc Specify® SureScan® MRI 5-6-5 grid, in-line spacing 4.5 mm, row spacing 1.0 mm, electrode size 4 mm
Implanted hemisphere	Right	Left and right
ECoG Grid location	Medial frontoparietal, covering M1 and S1, face and lip area	Left: Lateral frontoparietal, inferior parietal cortex and Broca (Brodmann area 44, inferior frontal gyrus pars opercularis left), Right: Medial frontoparietal, covering M1, S1 hand knob & PMDc
Total number of included electrodes	16	32
Number of electrodes over M1	3	Left: 2, Right: 3
Number of electrodes over S1	4	Left: 5, Right: 4

CGP. If none of the fingers are connected according to CGP, then each iteration step will consist of 5 BTTR blocks and Go-BTTR will evolve into a series of BTTR models as seen in figure 2, top panel. On the other hand, if all fingers are connected, and remain connected throughout subsequent iteration steps, then each iteration step will consist of a single eBTTR block and Go-BTTR will run exactly like eBTTR as seen in figure 2, bottom panel. Note that in the first iteration step of figure 3, the connection between the 2 fingers was labeled as bidirectional, but this is not always the case: if the connection is one-directional (e.g. matrix $\mathbf{Y}_1$ causes matrix $\mathbf{Y}_2$), then eBTTR would run on both fingers to produce a model for $\mathbf{Y}_2$, and regular BTTR would only use $\mathbf{Y}_1$. The overarching procedure is called graph-optimized block term tensor regression (Go-BTTR).

2.2.2. Go-BTTR: regression model

The proposed regression model is based on the BTD with automatic MTR determination, denoted as $(L_1^k, \ldots, L_N^k)$. This model employs a deflation-based

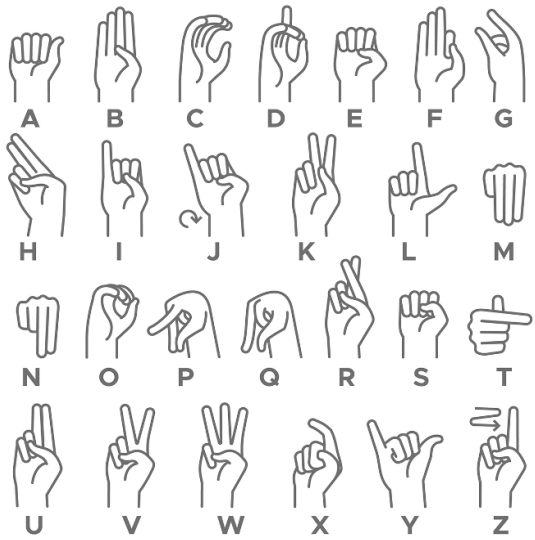

Figure 1. Flemish sign language alphabet [22] used in the Leuven experiment. Note that the 'D', 'F', 'V' and 'Y' signs of the American sign language alphabet, used in the Utrecht experiment, are identical to the corresponding Flemish signs.

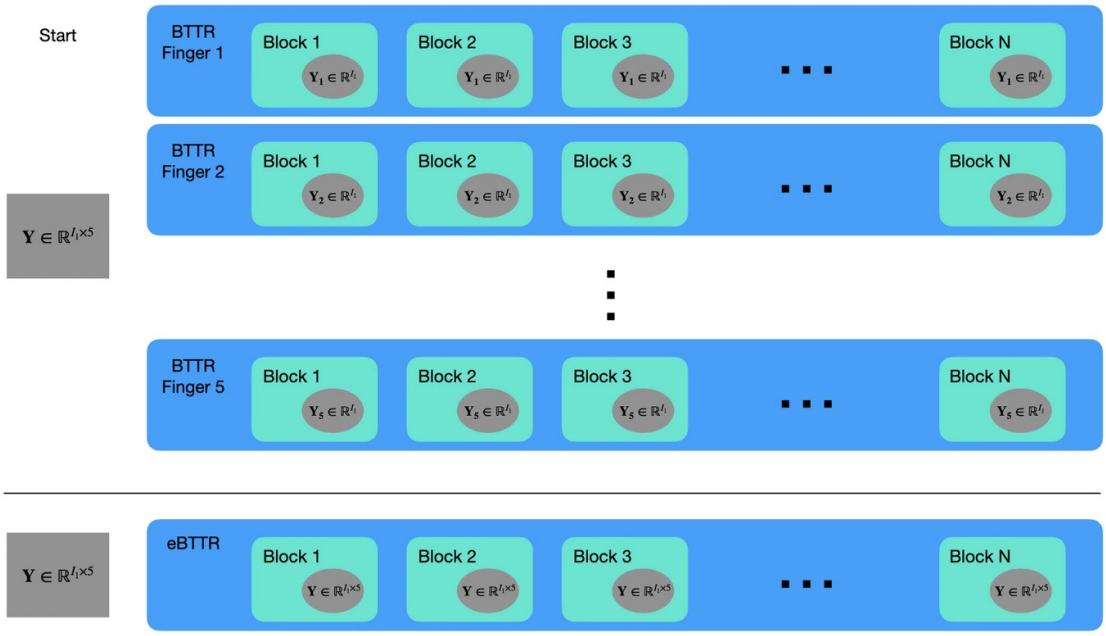

Figure 2. Scheme of BTTR (top panel) and eBTTR algorithm (bottom panel) with 2nd-order response variable **Y**.

approach to sequentially Tucker-decompose an ECoG tensor and a Finger Movement matrix into a sequence of blocks. Through the technique of ACE, each block comprises representations maximally correlated.

2.2.3. Go-BTTR: CGP model

The CGP has been developed to model and analyze unstructured data by applying signal processing techniques to graphs [20]. It provides a framework for inferring cause-effect relationships between the nodes of a graph, which we exploit here to detect which fingers should be joined in the next regression step.

The graph signal at time sample k is represented as follows:

$$x[k] = \begin{bmatrix} x_0[k] & x_1[k] & \cdots & x_{N-1}[k], \end{bmatrix}^T \in \mathbb{C}^N \quad (1)$$

with N the total number of nodes, K the total number of time samples, $x_n[k]$, a discrete time series of a node in a graph.

CGP is considered to be a discrete time series $x[k]$ on a graph of the following form [20]:

$$x[k] = w[k] + \sum_{i=1}^{M} P_i(A, c)$$

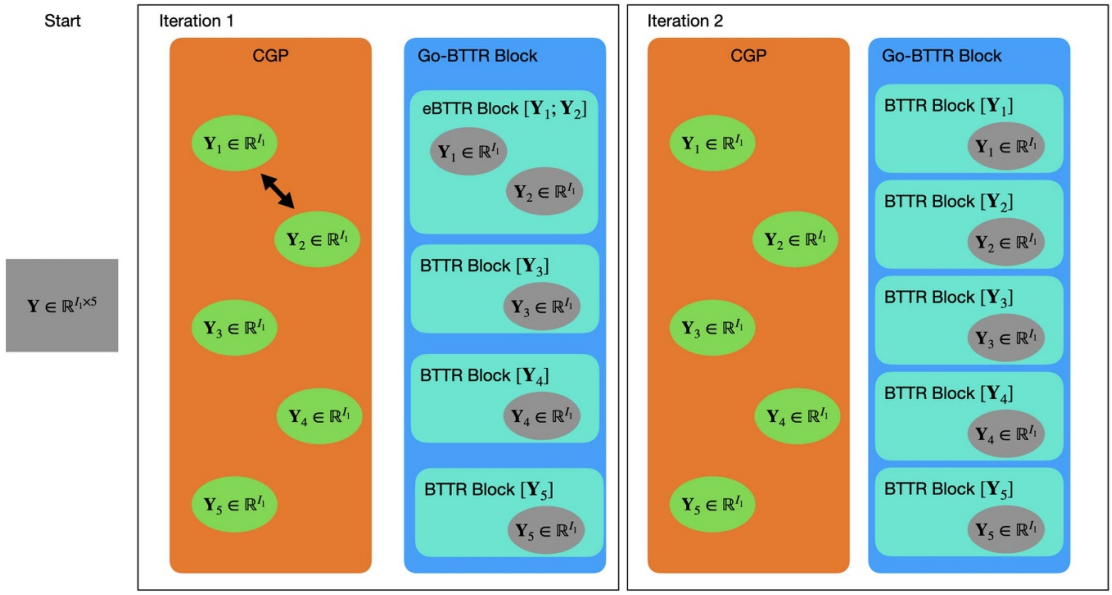

Figure 3. Scheme of Go-BTTR algorithm with 2nd-order response variable **Y**. Two iterations are shown, each one consisting of a CGP and a Go-BTTR step. See text.

$$x[k-i] = w[k] + \sum_{i=1}^{M} \left[\sum_{j=0}^{i} c_{ij}A^j\right] x[k-i] \times w[k] + (c_{10}I + c_{11}A)\,x[k-1] + \left(c_{20}I + c_{21}A + c_{22}A^2\right) x[k-2] + \ldots + \left(c_{M0}I + \ldots + c_{MM}A^M\right) x[k-M]$$

where $P_i(A,c)$ is a matrix polynomial in A, $w[k]$ statistical noise, c_{ij} a scalar polynomial coefficient, and

$$c = \begin{bmatrix} c_{10} & c_{11} & \cdots & c_{ij} & \cdots & c_{MM} \end{bmatrix}^T \qquad (2)$$

a vector collecting all the c_{ij}'s.

The CGP is a time series modeling technique rooted in autoregressive (Markov) processes. In this approach, the coefficients $P_i(A,c)$ are interpreted as graph filters. This constraint implies that the current value $x[k]$ at time step k cannot be influenced by network effects beyond the ith order, looking back i time steps. Additionally, this order is bounded by the minimum polynomial of the matrix A. [20].

The CGP model captures the finger interactions during a specific block which ensures that BTTR can focus on said interaction. Considering that BTTR constructs blocks with maximally correlated representations and the next block works with the remainder, the captured finger interactions will not be present in subsequent blocks.

2.3. Preprocessing

Notch filters, centered at 50 (as well as the second harmonic, 100) Hz, were used to eliminate power line noise. Afterwards, the data was visually examined to remove bad channels. A channel is considered bad if it exhibits an unstable signal (or unchanging signal). Subsequently, re-referencing with the application of common average reference (CAR) as described in [23]. At the end, a 4th-order tensor is constructed using the following approach:

- **Samples** follows the size of vector Y (which is recorded from the data glove).
- **Channels** are the amount of electrodes remaining after the removal of bad channels.
- **Frequencies** corresponds to 16 components, consisting of 15 gamma band amplitudes and the LMP. The gamma band amplitudes were extracted in the 60 to 130 Hz range (high-frequency bands) using 10 Hz frequency bands with a 5 Hz overlap. These were obtained using bidirectional third-order Butterworth band-pass filters [24]. The LMP was determined by extracting the power in the 0.1 to 1.5 Hz range.
- **Time** consists of 10 time instances derived from the most recent 1 s epoch, achieved by downsampling each of the eight band-pass filtered ECoG signals to 10 Hz.

The preprocessing occurs in the following manner:

- Normalize (z-score) data glove data independently for each finger $Y \in \mathbb{R}^{\text{Samples} \times \text{Fingers}}$
- For each channel, epoch selection is applied. For each sample, the previous second is used for band-pass filtering and then downsampled to 10 Hz, giving us the frequency and time dimensions for each sample and channel.

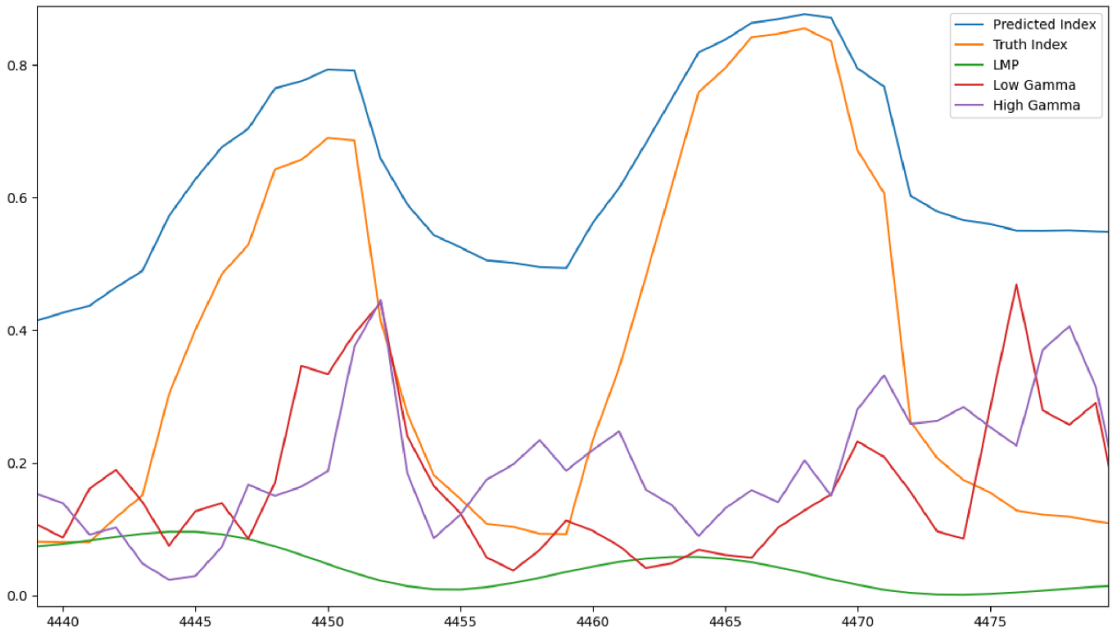

Figure 4. Raw recording of a single electrode for the activity of the index finger of subject 2 (Utrecht dataset) along with LMP, low and high gamma amplitude and the predicted trajectory (using Go-BTTR). *Y*-axis is in arbitrary units, *X*-axis in ms. Color of the curves as indicated in the insert.

- Normalize (z-score) tensor according to channel and frequency bands of the training set. The parameters for the z-scoring are used for the test set as well.
- Finally, the channel matrices are merged into a 4D tensor with dimensions of samples by channels by frequencies by time.

2.4. Evaluation metrics

The optimal number of blocks, denoted as K, for the Go-BTTR regression model, was determined by utilizing a five-fold cross-validation approach and a separate test set to determine model performance. Each dataset was split into a training, validation and testing set with a ratio of 60%, 20% and 20%, respectively. The training set was used to train the model, the validation set to determine the optimal number of blocks, and the test set to evaluate the model. Overfitting was avoided by using the validation set to determine the optimal number of blocks.

The evaluation of model performance relies on a correlation metric between the glove-recorded data and the predicted finger trajectories, in this case, Pearson correlation. The test dataset was partitioned into five non-overlapping blocks. For assessing the significance of differences in average accuracies across various fingers and subjects, we employed the significance was established using the Wilcoxon signed-rank test (two-tailed) based on a p-value, to indicate a difference in average accuracies across various fingers and subjects. A threshold of 0.05 was used. [25].

3. Results

3.1. Utrecht dataset

Figure 4 illustrates the relationship between the raw recordings, the ground truth (data glove), the features extracted from the ECoG data (frequency features, LMP, time features) and the predicted trajectory. figure 5 shows the connectivity matrix resulting from CGP in the first iteration step for Subject 2 of the Utrecht Data. We observe a substantial degree of self-connectivity, as expected, however we can see that the thumb, ring finger and pinky (labeled as 0, 1 and 4, respectively) exhibit a connection with other fingers. Since CGP rates connections on a continuous scale, a threshold has to be used. Experimentally, a threshold of 0.08 was used since in that case CGP reconstructs the original signal with at least 95% accuracy.

The results (as well as their standard deviations) are listed in table 3 for subjects 2, 3, 4 and 5, respectively. A box plot representation is shown in figure 6. Note that, as said above, data from subject 1 was not used as M1 was not covered.

Figure 7 graphs the Pearson correlation coefficient (y-axis), across all 4 gestures, as compared to the number of blocks (x-axis) used for each finger of subject 2 when using Go-BTTR. We see that the

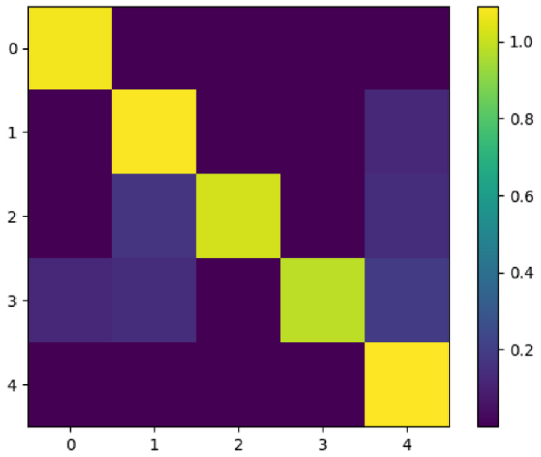

Figure 5. Connectivity of Subject 1 in the first iteration step (Utrecht dataset, 4 letters of the American sign language alphabet). The *x*-axis represents the 5 fingers and the *y*-axis the connected ones connected according to CGP in the first iteration step. The numbers 0 to 4 correspond to the Thumb, Index, Middle, Ring and Pinky.). The color intensity represents the strength of the connection in terms of Pearson correlation..

Table 3. Pearson correlation coefficients of cued finger gesture trajectories for Subjects 2, 3, 4, and 5 (Utrecht dataset, 4 letters of the American sign language alphabet). The average correlation across all fingers for all subjects was 0.73 for Go-BTTR, 0.719 for eBTTR and 0.70 for BTTR.

Methods	Fingers	Subject 2	Subject 3	Subject 4	Subject 5
Go-BTTR	Thumb	0.61 ± .06	0.51 ± .06	0.61 ± .06	0.61 ± .06
	Index	0.87 ± .09	0.57 ± .09	0.87 ± .09	0.87 ± .09
	Middle	0.85 ± .02	0.55 ± .02	0.85 ± .02	0.85 ± .02
	Ring	0.80 ± .04	0.70 ± .04	0.80 ± .04	0.80 ± .04
	Pinky	0.82 ± .02	0.42 ± .02	0.82 ± .02	0.82 ± .02
eBTTR	Thumb	0.62 ± .05	0.52 ± .03	0.62 ± .05	0.62 ± .05
	Index	0.87 ± .07	0.56 ± .05	0.87 ± .07	0.87 ± .07
	Middle	0.81 ± .04	0.51 ± .02	0.81 ± .04	0.81 ± .04
	Ring	0.80 ± .02	0.70 ± .02	0.80 ± .02	0.80 ± .02
	Pinky	0.80 ± .01	0.39 ± .01	0.80 ± .01	0.80 ± .01
BTTR	Thumb	0.58 ± .05	0.48 ± .05	0.58 ± .05	0.58 ± .05
	Index	0.85 ± .08	0.45 ± .08	0.85 ± .08	0.85 ± .08
	Middle	0.84 ± .04	0.54 ± .03	0.84 ± .04	0.84 ± .04
	Ring	0.79 ± .02	0.69 ± .02	0.79 ± .02	0.79 ± .02
	Pinky	0.72 ± .01	0.41 ± .02	0.72 ± .01	0.72 ± .01

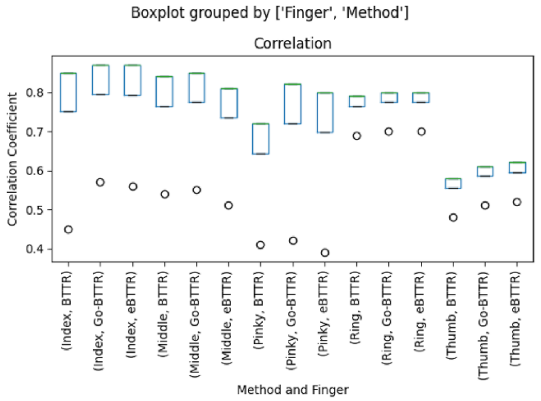

Figure 6. Pearson correlation coefficients of cued finger gesture trajectories for Subjects 2, 3, 4, and 5 (Utrecht dataset, 4 letters of the American sign language alphabet) in a box plot representation.

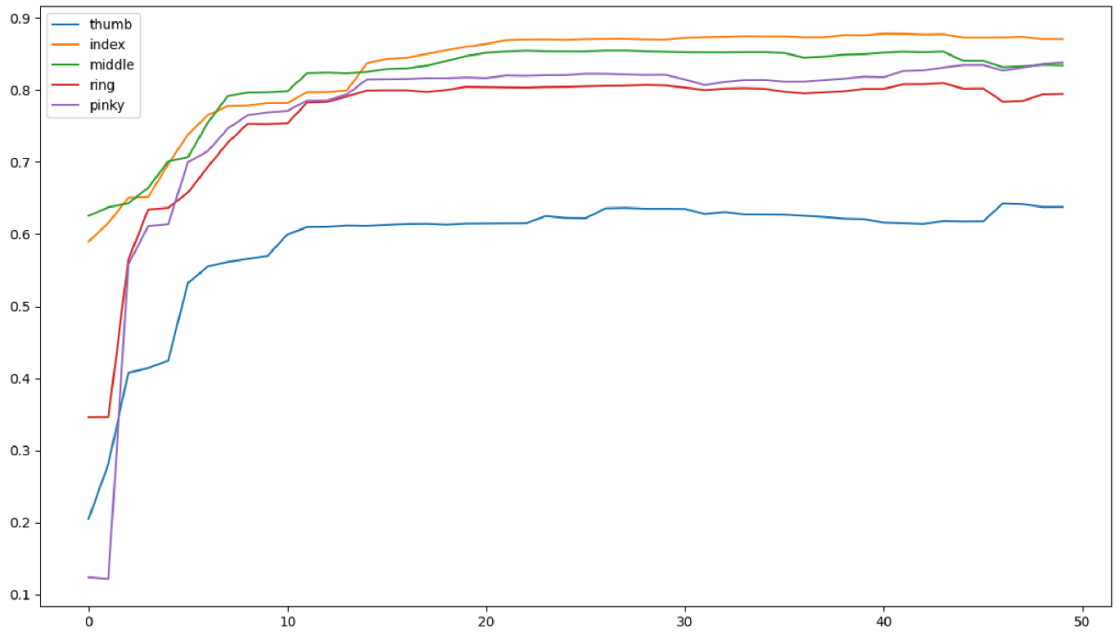

Figure 7. Pearson correlation coefficient, across all 4 gestures, compared to the number of blocks for each finger for subject 2 (Utrecht dataset). Finger color code as indicated in the insert.

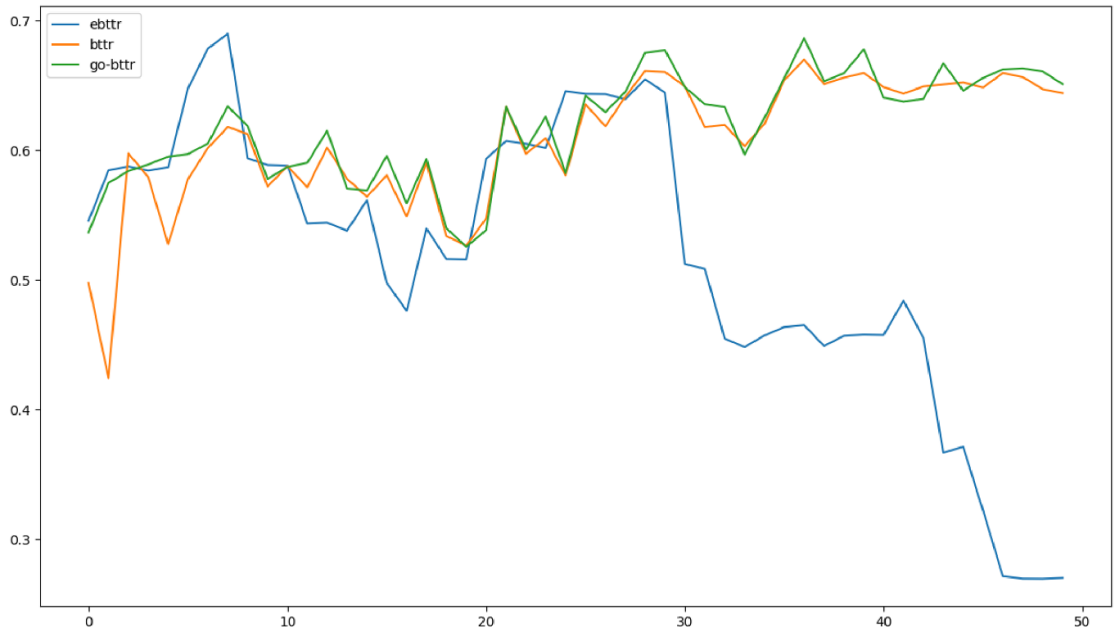

Figure 8. Pearson correlation coefficient (y-axis), across all gestures, of BTTR, eBTTR, and Go-BTTR compared to the number of blocks (x-axis) for the index finger of subject 2 (Utrecht dataset). Model color code as indicated in the insert. Note that the same eBTTR and Go-BTTR model is also used for the other fingers, while there are 5 separate models of BTTR (one for each finger).

accuracy generally increases as more blocks are used to eventually decrease slightly, as seen e.g. for the ring finger.

Figure 8 shows the Pearson correlation coefficient as compared to the number of blocks used for the index finger of subject 3 when using BTTR, eBTTR, and Go-BTTR. Both BTTR and Go-BTTR remain relatively stable as the number of blocks increases whereas eBTTR is less stable as it exhibits more significant lapses in performance. The likely cause is that, from a certain number of block onwards, various fingers within eBTTR become independent.

Figure 9 shows a still image of a hand avatar performing the movements predicted by Go-BTTR.

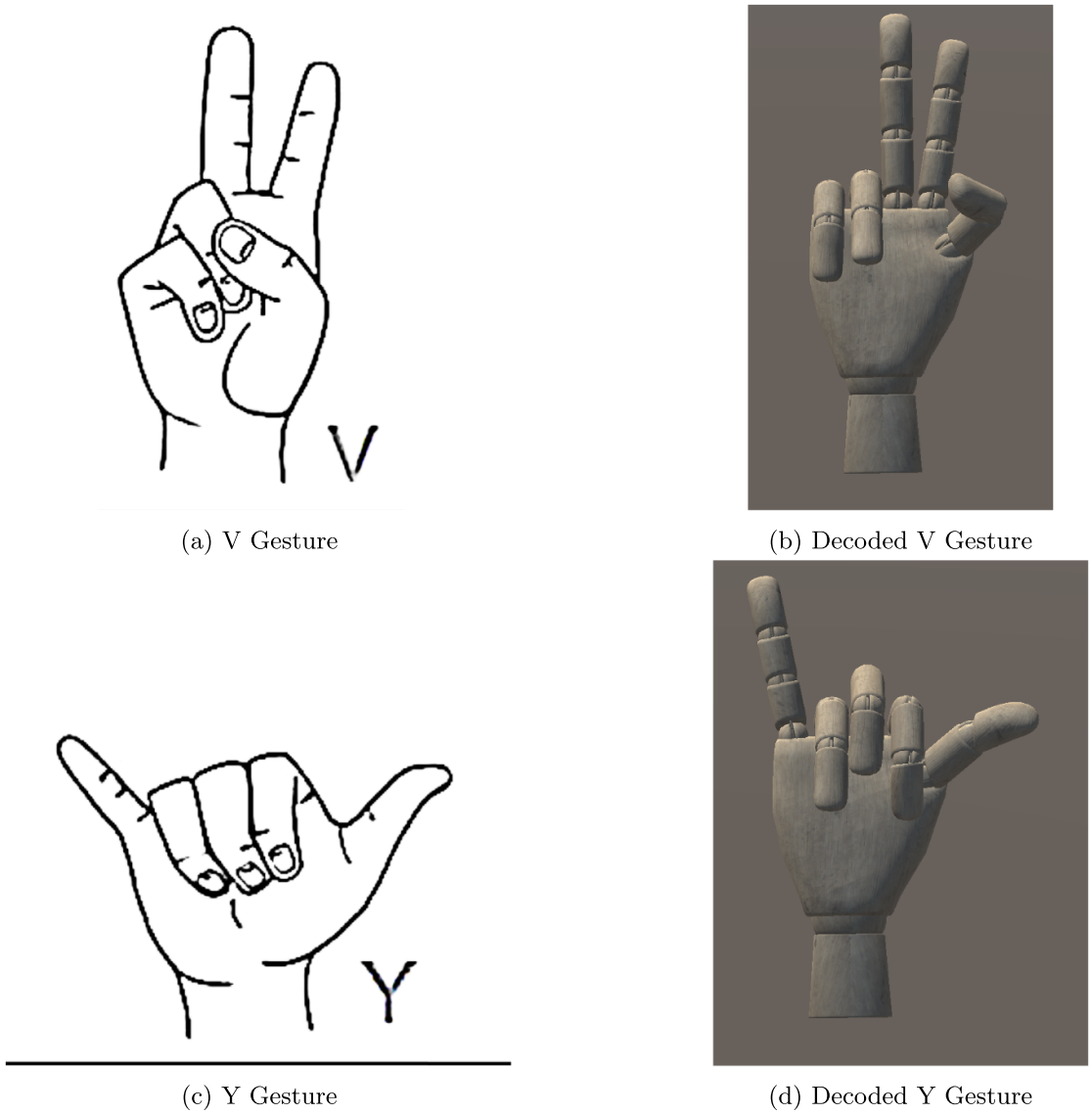

(a) V Gesture (b) Decoded V Gesture

(c) Y Gesture (d) Decoded Y Gesture

Figure 9. Cued (left panels) and decoded gestures (right panels) of subject 3, Utrecht dataset.

We observe that the predicted movement is visually rECOGnizable as the intended gesture. On the other hand, figure 10 shows the finger flexions for the Y gesture of the ground truth (data glove) and Go-BTTR prediction for all fingers of subject 2. We observe that the predicted finger flexions are in line with the ground truth.

3.2. Leuven dataset

The results for Task 1 are listed in table 4 for subject 1. We observe that Go-BTTR significantly outperforms eBTTR for the index and middle fingers and BTTR for the ring finger, and is on par with the best finger performances. Similar to the Utrecht data set, there is also the issue of stability of the deflation process. Figure 11 shows that, for the index finger of subject 1, Go-BTTR remains as stable as BTTR when the number of blocks increases whereas eBTTR is less stable and develops a significant decrease in performance. The likely cause is that, beyond a certain number of blocks, the various targets within eBTTR become independent.

Task 2 considers all gestures of the sign language alphabet, thus going beyond the selection of 4 gestures as in the Utrecht experiment. The results, represented in the form of Pearson correlation coefficients, are given in table 5 for subjects 1 and 2, respectively. A box plot representation is shown in figure 12.

For subject 1 we observe for the middle finger and pinky a statistically significant lower performance for eBTTR compared to Go-BTTR. On the other hand, for subject 2, the index finger, ring finger and pinky exhibit statistically significantly lower performance for BTTR compared to Go-BTTR. This shows that, depending on subject and finger, either BTTR or eBTTR perform better, but that Go-BTTR, due to its connectivity model, manages to consistently yield the best performance.

The decoders applied to the Leuven dataset exhibit significantly lower correlation coefficients

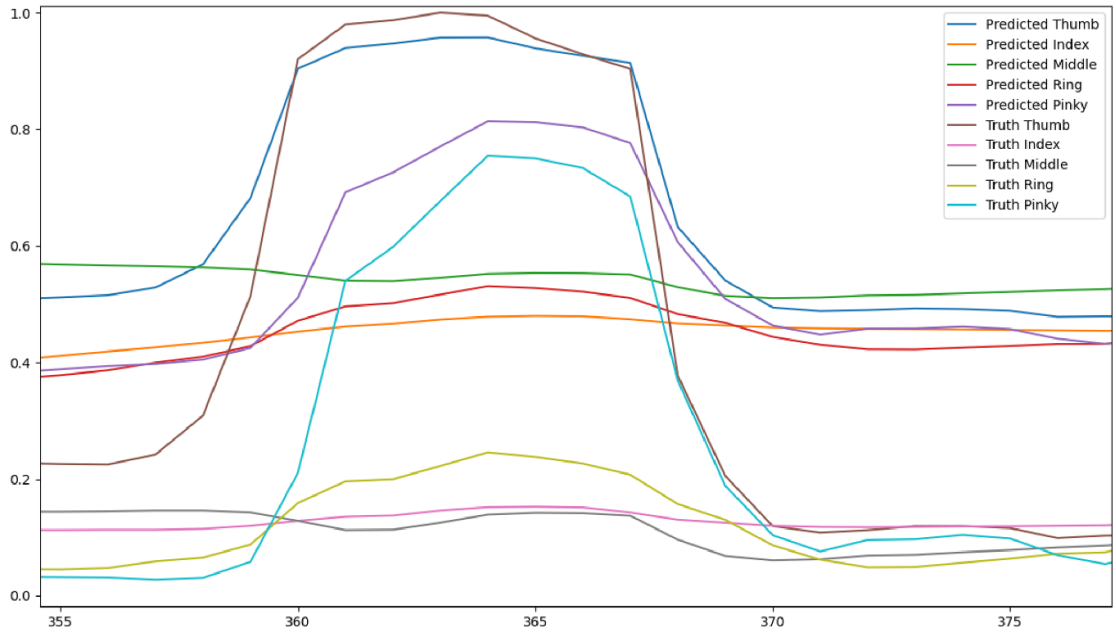

Figure 10. Finger flexions, for the Y gesture, of the ground truth (data glove) and Go-BTTR prediction for all fingers of subject 2 (Utrecht dataset). *Y*-axis is in arbitrary units, *x*-axis in ms. Color code as indicated in the insert.

Table 4. Pearson correlation coefficients of cued single-finger movement trajectories of Subject 1 (Task 1, Leuven dataset). Significantly different results compared Go-BTTR are indicated in bold.

Methods	Thumb	Index	Middle	Ring	Pinky
Go-BTTR	0.32 ± .06	0.55 ± .09	0.48 ± .02	0.23 ± .04	0.18 ± .02
eBTTR	0.31 ± .05	**0.45 ± .07**	**0.12 ± .04**	0.23 ± .02	0.16 ± .01
BTTR	0.32 ± .05	0.55 ± .08	0.47 ± .04	**0.17 ± .02**	0.17 ± .01

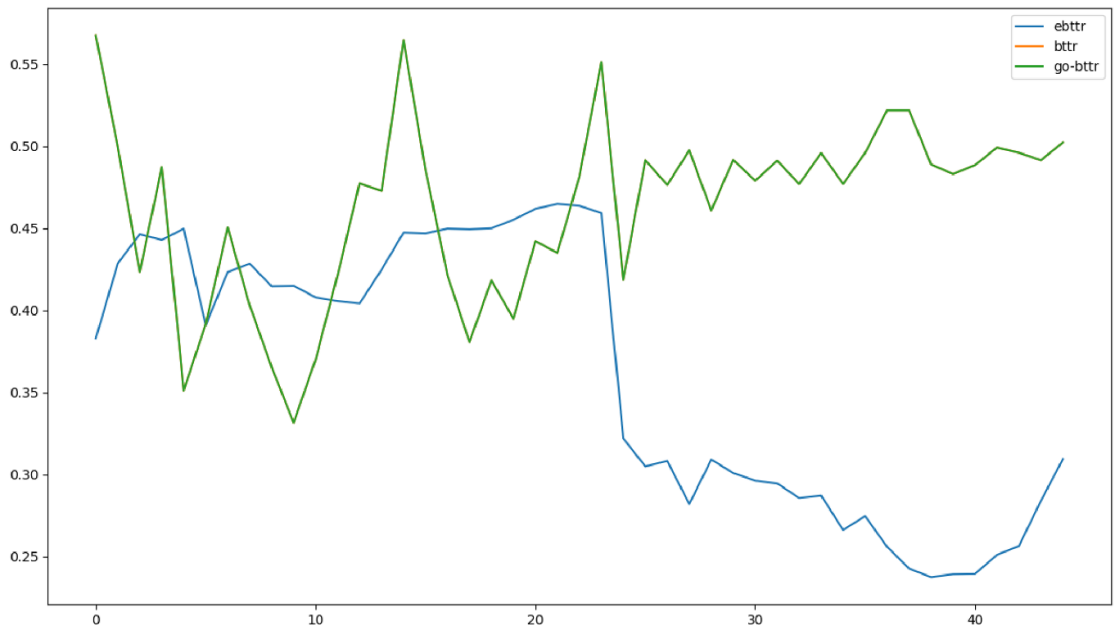

Figure 11. Pearson correlation coefficient (*y*-axis) compared to the number of blocks (*x*-axis) for the index finger for subject 1 (Task 1, single-finger trajectories, Leuven data set). Note that the performance of Go-BTTR coincides with that of BTTR. This is because Go-BTTR detects that only finger is moving, defaulting Go-BTTR to BTTR. .

Table 5. Pearson correlation coefficients of cued finger gesture trajectories for Subject 1 and Subject 2 (Task 2, 26 letters of the Flemish sign alphabet, Leuven dataset). Bold values indicate significantly different results compared to Go-BTTR. The average correlation across all fingers for all subjects was 0.37 for Go-BTTR, 0.34 for eBTTR and 0.33 for BTTR.

Methods	Fingers	Subject 1	Subject 2
Go-BTTR	Thumb	0.42 ± .06	0.32 ± .06
	Index	0.36 ± .09	0.46 ± .09
	Middle	0.48 ± .02	0.55 ± .02
	Ring	0.23 ± .04	0.32 ± .04
	Pinky	0.18 ± .02	0.33 ± .02
eBTTR	Thumb	0.42 ± .05	0.32 ± .05
	Index	0.32 ± .07	0.46 ± .07
	Middle	**0.38 ± .04**	0.49 ± .04
	Ring	0.23 ± .02	0.32 ± .02
	Pinky	**0.12 ± .01**	0.33 ± .01
BTTR	Thumb	0.38 ± .05	0.28 ± .05
	Index	0.36 ± .08	**0.41 ± .08**
	Middle	0.47 ± .04	0.55 ± .04
	Ring	0.23 ± .02	**0.23 ± .02**
	Pinky	0.17 ± .01	**0.24 ± .01**

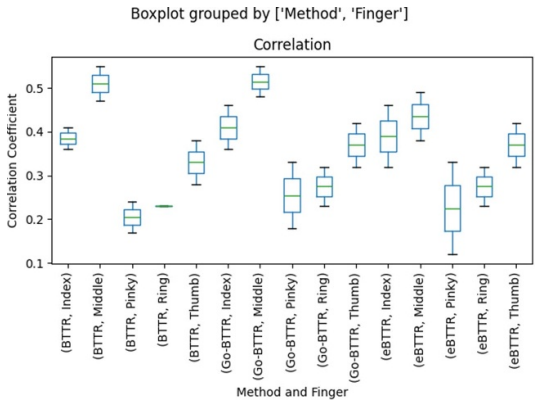

Figure 12. Pearson correlation coefficients of cued finger gesture trajectories for Subject 1 and Subject 2 (Task 2, 26 letters of the Flemish sign alphabet, Leuven dataset) in a box plot representation.

compared to the Utrecht dataset. This is because the Leuven dataset was recorded with epidural electrodes whereas the Utrecht dataset with subdural electrodes. Epidural recordings exhibit lower signal amplitudes than their subdural counterpart, particularly when using high-density grids, and this can lead to lower finger trajectory correlations ([26]). However, as with Go-BTTR finger the correlation coefficients converge consistently for both datasets, as shown in figures 6 and 8, we can conclude that the proposed method is robust to the quality of the data.

Figure 13 shows the finger flexions for the Y gesture of the ground truth and Go-BTTR prediction for all fingers of subject 2. We observe that the predicted finger flexions are in line with the ground truth despite the lower correlation coefficients.

3.3. Computational complexity

Because of CGP, Go-BTTR is computationally more expensive than BTTR or eBTTR. However, Go-BTTR assumes that finger connectivity either remains constant or decreases with increasing number of blocks. In the worst case, finger connectivity remains constant, and CGP needs to run on the connected fingers every block. In the best case, as fingers become more independent, a smaller number of finger configuration need to be exploited, thereby saving on CGP computations.

On a Macbook Pro M1 2020 with 16GB of RAM, the training time for Go-BTTR was 28 minutes for the Utrecht dataset and 34 minutes for the Leuven dataset (Task 1, single-finger flexion). The training time for BTTR was 13 minutes for the Utrecht dataset and 16 minutes for the Leuven dataset. The training time for eBTTR was 18 minutes for the Utrecht dataset and 22 minutes for the Leuven dataset.

4. Conclusion

With tensor-based decoders, multiway structured data can be better exploited than by relying on data unfolding [27]. Decoding joint finger movement

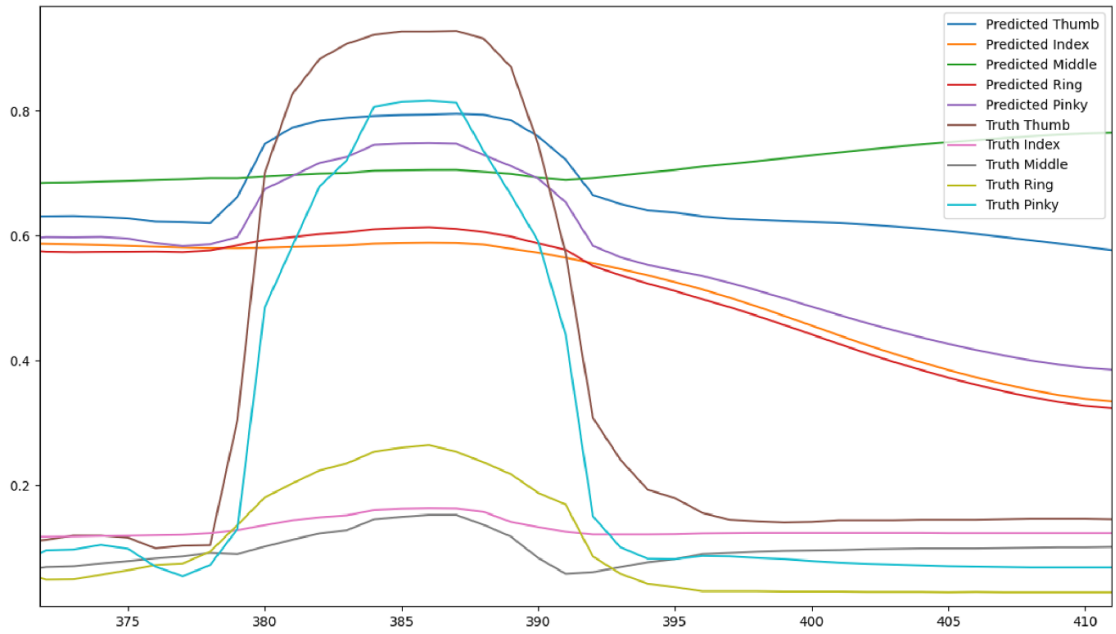

Figure 13. Finger flexions for the Y gesture of the ground truth and Go-BTTR prediction for all fingers of subject 2 (Task 2, 26 letters of the Flemish sign alphabet, Leuven dataset). *Y*-axis is in arbitrary units, *x*-axis in ms. Color code as indicated in the insert.

trajectories and particularly sign language gestures from ECoG recordings is a challenging task but needed when envisaging dexterity in BCI-based applications. However, for hand prosthetic- or exoskeleton settings during realistic object handling, decoding of complex finger movement trajectories is necessary. To solve this, we proposed a novel approach that extends the block term tensor regression approach developed before by introducing CGP to account for fingers that become connected when performing coordinated movements. In this way, Go-BTTR serves as an optimal middle ground giving the best of both BTTR and its extension, eBTTR. Thereby preserving the coordinated finger performance of eBTTR, while retaining the single-finger stability of BTTR.

Data availability statement

The data cannot be made publicly available upon publication because they contain sensitive personal information. The data that support the findings of this study are available upon reasonable request from the authors.

Funding

AF was supported by the Belgian Fund for Scientific Research—Flanders (FWO 1157 019 N). MMVH is supported by research grants received from the European Union's Horizon 2020 research and innovation programme under grant agreement No. 857 375, the special research fund of the KU Leuven (C24/18/098), the Belgian Fund for Scientific Research—Flanders (G0A4118N, G0A4321N, G0C1522N), and the Hercules Foundation (AKUL 043).

ORCID iDs

Axel Faes https://orcid.org/0000-0002-1637-255X
Eva Calvo Merino https://orcid.org/0000-0002-8782-3856
Mariana P Branco https://orcid.org/0000-0002-7316-8846
M M Van Hulle https://orcid.org/0000-0003-1060-7044

References

[1] Who spinal cord injury (available at: www.who.int/news-room/fact-sheets/detail/spinal-cord-injury) (Accessed 30 June 2022)
[2] Eliza de Oliveira Schultz Ascari R, Pereira R and Silva L 2018 Mobile interaction for augmentative and alternative communication: a systematic mapping *J. Interact. Syst.* **9**
[3] Lorach H, Galvez A, Spagnolo V, Martel F, Karakas S, Intering N, Vat M, Faivre O, Harte C and Komi S *et al* 2023 Walking naturally after spinal cord injury using a brain–spine interface *Nature* **618** 1–8
[4] Hochberg L R, Serruya M D, Friehs G M, Mukand J A, Saleh M, Caplan A H, Branner A, Chen D, Penn R D and Donoghue J P 2006 Neuronal ensemble control of prosthetic devices by a human with tetraplegia *Nature* **442** 164–71
[5] Collinger J L, Wodlinger B, Downey J E, Wang W, Tyler-Kabara E C, Weber D J, McMorland A J, Velliste M, Boninger M L and Schwartz A B 2013 High-performance neuroprosthetic control by an individual with tetraplegia *Lancet* **381** 557–64
[6] Hochberg L R *et al* 2012 Reach and grasp by people with tetraplegia using a neurally controlled robotic arm *Nature* **485** 372–5
[7] Wodlinger B, Downey J E, Tyler-Kabara E C, Schwartz A B, Boninger M L and Collinger J L 2014 Ten-dimensional anthropomorphic arm control in a human brain- machine

interface: difficulties, solutions and limitations *J. Neural Eng.* **12** 016011
[8] Anderson N R, Blakely T, Schalk G, Leuthardt E C and Moran D W 2012 Electrocorticographic (ECOG) correlates of human arm movements *Exp. Brain Res.* **223** 1–10
[9] Ball T, Kern M, Mutschler I, Aertsen A and Schulze-Bonhage A 2009 Signal quality of simultaneously recorded invasive and non-invasive EEG *Neuroimage* **46** 708–16
[10] Bundy D T, Pahwa M, Szrama N and Leuthardt E C 2016 Decoding three-dimensional reaching movements using electrocorticographic signals in humans *J. Neural Eng.* **13** 026021
[11] Bleichner M G, Freudenburg Z V, Martijn Jansma J M, Aarnoutse E J, Vansteensel M J and Franciscus Ramsey N F 2016 Give me a sign: decoding four complex hand gestures based on high-density ECOG *Brain Struct. Funct.* **221** 203–16
[12] Li Y, Zhang S, Jin Y, Cai B, Controzzi M, Zhu J, Zhang J and Zheng X 2017 Gesture decoding using ECOG signals from human sensorimotor cortex: a pilot study *Behav. Neurol.* (https://doi.org/10.1155/2017/3435686)
[13] Pan G, Li J-J, Qi Y, Yu H, Zhu J-M, Zheng X-X, Wang Y-M and Zhang S-M 2018 Rapid decoding of hand gestures in electrocorticography using recurrent neural networks *Front. Neurosci.* **12** 555
[14] Zhao Q, Caiafa C F, Mandic D P, Chao Z C, Nagasaka Y, Fujii N, Zhang L and Cichocki A 2012 Higher order partial least squares (HOPLS): a generalized multilinear regression method *IEEE Trans. Pattern Anal. Mach. Intell.* **35** 1660–73
[15] Eliseyev A, Aksenova T and Zhang D 2016 Penalized multi-way partial least squares for smooth trajectory decoding from electrocorticographic (ECOG) recording *PLoS One* **11** e0154878
[16] Louis Benabid A L *et al* 2019 An exoskeleton controlled by an epidural wireless brain–machine interface in a tetraplegic patient: a proof-of-concept demonstration *Lancet Neurol.* **18** 1112–22
[17] Camarrone F, Branco M P, Ramsey N F and Van Hulle M M 2020 Accurate offline asynchronous detection of individual finger movement from intracranial brain signals using a novel multiway approach *IEEE Trans. Biomed. Eng.* **68** 2176–87
[18] Faes A, Camarrone F and Van Hulle M M 2022 Single finger trajectory prediction from intracranial brain activity using block-term tensor regression with fast and automatic component extraction *IEEE Trans. Neural Netw. Learn. Syst.* submitted
[19] Faes A and Van Hulle M M 2022 Finger movement and coactivation predicted from intracranial brain activity using extended block-term tensor regression *J. Neural Eng.* **19** 066011
[20] Mei J and Moura J M F 2016 Signal processing on graphs: causal modeling of unstructured data *IEEE Trans. Signal Process.* **65** 2077–92
[21] Branco M P, Freudenburg Z V, Aarnoutse E J, Bleichner M G, Vansteensel M J and Ramsey N F 2017 Decoding hand gestures from primary somatosensory cortex using high-density ECOG *NeuroImage* **147** 130–42
[22] Filip Heyninck vlaams alphabet gebarentaal (available at: www.filipheyninck.com/illustraties) (Accessed 24 April 2023)
[23] Binnie C D 2003 *Clinical neurophysiology: EEG, paediatric neurophysiology Special Techniques and Applications* vol 2 (Elsevier Health Sciences)
[24] Tucker L R 1966 Some mathematical notes on three-mode factor analysis *Psychometrika* **31** 279–311
[25] Wilcoxon F 1992 Individual comparisons by ranking methods *Breakthroughs in Statistics* (Springer) pp 196–202
[26] Branco M P, Geukes S H, Aarnoutse E J, Ramsey N F and Vansteensel M J 2023 Nine decades of electrocorticography: a comparison between epidural and subdural recordings *Euro. J. Neurosci.* **57** 1260–88
[27] Cichocki A, Mandic D, Caiafa C, Phan A H, Zhou G, Zhao Q and De Lathauwer L 2015 Multiway component analysis: tensor decompositions for signal processing applications *IEEE Signal Process. Mag.* **32** 145–63